Elsevier Editorial System(tm) for Composites Part B
Manuscript Draft

Manuscript Number: JCOMB-D-14-00863R1

Title: Polydimethylsiloxane-barium titanate composites: preparation and evaluation of the morphology, moisture, thermal, mechanical and dielectric behavior

Article Type: Full Length Article

Keywords: A. Polymer-matrix composites (PMCs); A. Smart materials; B. Electrical properties; D. Mechanical testing

Corresponding Author: Dr. Maria Cazacu, Ph.D.

Corresponding Author's Institution: "Petru Poni" Institute of Macromolecular Chemistry

First Author: Adrian Bele

Order of Authors: Adrian Bele; Maria Cazacu, Ph.D.; George Stiubianu; Stelian Vlad; Mircea Ignat

Abstract: Polydimethylsiloxane-alpha, omega-diols were used as matrix for barium titanate particles to obtain electroactive elastomeric composites. Filler particles were previously treated with a surfactant to improve the compatibility with and dispersability in the matrix. The composites, processed as films and crosslinked with methyltriacetoxysilane, were investigated from point of view of the morphology, moisture sorption and thermal properties, as well as mechanical and dielectric behavior. Maximum strain value of 850% at 0.32 MPa and dielectric permittivity of 4.41 at 10 Hz and 20 ºC were obtained. Two parameters of interest for potential future application of such materials in electromechanical devices (actuation or harvesting), electromechanical sensitivity and harvesting energy capacity, were estimated and discussed in correlation with the molecular mass of the polymeric matrix and the content of the active filler.

Polydimethylsiloxane-barium titanate composites: preparation and evaluation of the morphology, moisture, thermal, mechanical and dielectric behavior

Adrian Bele[a], Maria Cazacu[a*], George Stiubianu[a], Stelian Vlad[a], Mircea Ignat[b]

[a] *"Petru Poni" Institute of Macromolecular Chemistry, Aleea Gr. Ghica Voda 41A, 700487 Iasi, Romania*

[e] *National Institute for Research and Development in Electrical Engineering ICPE-CA, 313 Splaiul Unirii, Bucharest,* 030138, *Romania*

Abstract

Polydimethylsiloxane-α,ω-diols were used as matrix for barium titanate particles to obtain electroactive elastomeric composites. Filler particles were previously treated with a surfactant to improve the compatibility with and dispersability in the matrix. The composites, processed as films and crosslinked with methyltriacetoxysilane, were investigated from point of view of the morphology, moisture sorption and thermal properties, as well as mechanical and dielectric behavior. Maximum strain value of 850% at 0.32 MPa and dielectric permittivity of 4.41 at 10 Hz and 20 ºC were obtained. Two parameters of interest for potential future application of such materials in electromechanical devices (actuation or harvesting), electromechanical sensitivity and harvesting energy capacity, were estimated and discussed in correlation with the molecular mass of the polymeric matrix and the content of the active filler.

Keywords: A. Polymer-matrix composites (PMCs); A. Smart materials; B. Electrical properties; D. Mechanical testing

1. Introduction

Silicone rubber is a well-known dielectric elastomer which is used in electromechanical transducers, devices able to convert electrical energy into mechanical one and vice versa [1]. A promising application of these materials, which is currently being investigated, is the generation of electricity from ocean waves energy [2,3]. For such applications, large displacement with high precision and speed are required, together with durability and reliability. In order to obtain high actuation strain, a material with low

* To whom correspondence will be addressed, e-mail: mcazacu@icmpp.ro

stiffness (low Young's modulus), high breakdown strength, and high permittivity is desired [4]. Silicones have highly desired elastic behaviour, their representative polydimethylsiloxane (PDMS) being known for its unusual rheological/flow properties [5]. The polarizability of the Si-O bond that constitutes a premise for a high dielectric constant is higher as compared to organic nonpolar polymers (e.g., polyethylene), but in reality, this is not so much due to the side methyl groups (in the case of PDMS), which prevent Si-O dipoles from approaching each other too closely) [6]. In order to increase the dielectric constant, the polysiloxanes are chemically modified by attaching polar groups, such as N-Allyl-N-methyl-4-nitroaniline [7], cyanalkyl [8], etc. to the silicon atoms. Fillers are often used to enhance the dielectric as well as the mechanical properties of the silicones [9]. The use of high permittivity inorganic fillers is a well-established technique to improve the dielectric constant of a polymer matrix. Various permittivity values can be achieved by changing the type and percentage of the filler in the substrate. Based on the literature data, it can be identified mainly three types of filler used to improve the permittivity of the dielectric elastomer actuator: ceramic particles with a high dielectric constant, such as titanium dioxide, barium titanate, magnesium niobate, lead magnesium niobate–lead titanate, and strontium titanate [9-13]; conductive particles, such as carbon nanotube, carbon black, copper–phthalocyanine/polyaniline [14] and short fibers [11]; highly polarizable conjugated polymer, such as undoped poly(3-hexyltiophene), polyaniline, polythiophene incorporated by blending or as nanoparticles [9,11]. $BaTiO_3$, a ferroelectric crystal which exhibits spontaneous polarization and high electrical breakdown strength is often used in this aim [15]. Thus, it has been incorporated in different polymeric matrix [12], like epoxides, polystyrenes [16], polyimides, polyetherimides [17], poly-ethylene-glycol-diacrylate (PEGDA) [18], polyurethane [19], acrylics [20,21], etc. This was also used as filler for PDMS [22]. The effect of $BaTiO_3$ nanoparticles on electrical and mechanical properties were extensively studied and found that dielectric constant of nanocomposites increases significantly with the increase in $BaTiO_3$ concentration where as the volume resistivity decreases continuously [22]. Commercially available barium titanate with particles of different shape and size or prepared by certain procedure to obtain a certain size and shape were used [23,24]. There are a few commercial dielectric elastomer materials available, these mainly including acrylic VHB (Very High Bond – a 3M tape) foil, silicones, polyurethanes, and some polystyrene/polybutadiene copolymers, acrylics and acrylonitrile butadiene rubber [13,25]. In general, commercially available room temperature vulcanization formulations based on low molecular weight

polydimethylsiloxane were used as matrix in such cases and either addition (hydrosilylation) or condensation (with tetrafunctional silanes) mechanisms were used to convert the fluid compounds in silicone elastomers.

Different from the literature, in this paper, home prepared PDMSs of different molecular masses, higher as compared with those used in other studies, were used as polymeric matrix in which surface-treated barium titanate was incorporated in different percents. The composites were processed as films and crosslinked by condensation at room temperature with a trifunctional silane, methyltriacetoxysilane. The morphology, moisture sorption, thermal, mechanical and dielectric properties were investigated.

2. Experimental

2.1. Materials

The polydimethylsiloxane-α,ω-diols, PDMSs, were synthesized according to the already described procedure [26]: cationic ring-opening polymerization of octamethylcyclotetrasiloxane in the presence of a cation exchanger as catalyst. Molecular masses were estimated on the basis of GPC analysis as being those presented in Table 1. Barium titanate ($BaTiO_3$), CO, with particle size < 3μm according to supplier (Fluka AG) was investigated through SEM and TEM to determine the particle size and shape (Figure 1ESI), while BET area (11.419 m^2/g) we estimated on the basis of water vapour sorption isotherms registered in dynamic regime (Figure 2ESI) and PLURONIC L-31, HO-poly(ethyleneglycol)-*block*-poly(propyleneglycol)-*block*-poly(ethyleneglycol)-OH (M=1100, d^{25}_{25} = 1.02, PEG, 10 wt. %) were purchased Fluka AG. Methyltriacetoxysilane (MTAS) was prepared and purified in house (b.p. =94-95 ^oC, d_4^{20} = 1.20).

2.2. Equipments

GPC measurements were made in $CHCl_3$ on a PL-EMD 950 Chromatograph - Evaporative Mass Detector. The calibration was performed with polystyrene standards.

For SEM studies, the as obtained thick films (foils) were cryo-fractured and the cross-section surface was examined with an Environmental Scanning Electron Microscope (ESEM) type Quanta 200, operating at 30 kV with secondary electrons in low vacuum mode. Dynamic water vapor sorption (DVS) capacity of the samples was determined in the relative humidity (RH) range 0–90% by using the fully automated gravimetric analyzer IGAsorp produced by Hiden Analytical, Warrington (UK). Thermogravimetric (TG)

measurements were conducted on a STA 449 F1 Jupiter device (Netzsch, Germany) in nitrogen atmosphere, in the temperature range 25 - 700^{o}C at a heating rate of 10 ^{o}C min^{-1}. DSC measurements were conducted with a DSC 200 F3 Maia (Netzsch, Germany in nitrogen atmosphere at a heating rate of 10 ^{o}Cmin^{-1}. Stress–strain measurements were performed on TIRA test 2161 apparatus, Maschinenbau GmbH Ravenstein, Germany on dumbbell-shaped cut samples with dimensions of 50x8.5x4 mm. Measurements were run at an extension rate of 20 mm/min, at room temperature. All samples were measured three times and the averages of the obtained values were taken into consideration. The acquired data were processed with MatLab software. Cyclic tensile stress tests were performed on the similar samples between 2 and 100% strain. The maximum force applied was tensile stress value as determined by previously test. Five stretch–recovery cycles were registered. The stationary time at minimum and maximum applied stress was 5 s. Dielectric spectra were registered on a Novocontrol "Concept 40" broadband dielectric spectrometer (Hundsangen, Germany), at room temperature in the frequency domain 1 Hz–1 MHz. Dielectric strength measurements were made at PERCRO Laboratory - TeCIP Institute - Scuola Superiore Sant'Anna, Pisa, Italy, on a home-made installation consisting in an USB-based oscilloscope, a signal generator and a direct current (DC) four-quadrant high-speed HV power amplifier with ±10kV and ±10mA voltage and current ratings. Brass electrodes were used to obtain breakdown voltage. The High-Voltage cylindrical electrode is 25 mm in diameter and 25 mm high. The grounded electrode is 15 cm in width and 75 cm in length. After the samples were placed on the grounded electrode, a polycarbonate frame was attached and clamped to ensure compliant contact between samples and electrodes. The HV electrode was placed in the hole from the polycarbonate frame and the maximum voltage was measured. The tests were made at 60 Hz and a 2000 V/s rate of voltage increase. The experiments were performed at room temperature and the surrounding medium was air. All the tested samples were brought into equilibrium with the atmospheric humidity. The harvesting tests were performed on a home-made set-up (Figure 3ESI) [27]. Electrodes of dimensions 20x20mm made of simple sticlotextolit (glass fibers impregnated with formaldehyde resin) plated with copper were placed on both sides of the sample. The connecting wires were attached to the electrodes by soldering and were connected to the measurement terminals of an oscilloscope Tektronix DPO4032 (350MHz, 2,5GS/s). A steel ball (m = 7.1 g) was left to fall freely from a height of 100 mm in the center of the upper electrode surface. The signal wave form and the voltage levels corresponding for the peaks at the impact of the ball

on contact surface of the sensor were monitored and were acquired (Figure 4ESI). More sets of measurements there have been done for each sample, finally being considered more representative three results for each.

2.3. Procedure

Pre-established amounts of barium titanate microparticles were mixed with surfactant PLURONIC L-31 then chloroform was added to obtain a less viscous mixture which was transferred over PDMS. Then MTAS, as crosslinker (Table 1), was added and stirred thoroughly until the components formed a homogenous mixture. The resulted mixture was sonicated for 10 minutes in order to remove all the air bubbles trapped in the mixture and then was used to obtain thin films (of about 0.5-1 mm thickness) by pouring in a teflon mold (15x5 cm). The samples were maintained in air at room temperature for 24 h and subsequently the formed films were easy peeled off from the substrate. The films were then kept in the laboratory environment about two weeks for aging before characterization by different techniques.

3. Results and discussions

PDMSs of different molecular masses were used as a matrix for the incorporation of different amounts of barium titanate, according to Table 1. Commercial barium titanate (with particles <3 μm in overall dimensions) was used in this study. The main difficulties concerning to the incorporation of such fillers in the silicone matrix are due to the known low compatibility of the silicones with almost any organic or inorganic partner. The improvement of the fillers compatibility with the polymer matrix can be achieved by surface functionalization through such methods as oxidation, heat and chemical treatment, vapor deposition, or coating with a third component such as surfactants, coupling agents, or grafted polymers [15,28]. In this paper we used a surfactant, Pluronic L-31, and the incorporation of the treated particles within polymeric matrix was performed by dispersive (incorporation, wetting and stabilization of the filler microparticles against later agglomeration) and extensive (distribution of filler particles within matrix) mixing mechanisms [28]. After homogenization, and deaeration, the mixture was poured in film on Teflon substrate. Under the atmospheric humidity, the crosslinking occurs, according to Scheme 1, with the formation of a dimensional stable film. The homogeneous films obtained were transparent to white opaque depending on the filler content (Figure 5ESI).

Table 1

Scheme 1

Figure 1

By examining SEM images (Figure 1), it can be seen spheres spread within the continuous polymeric matrix. These consist in surfactant volume incorporating ceramic particles. While the dimension of used barium titanate particles is of few micrometers (Figure 1ESI), the aggregates within composite are slightly larger than 10 micrometers with high polydispersity (i.e., 3-16 micrometer). Thus, it seems that, in the chosen working conditions, the effect of the surfactant is not the one expected. Maybe the ultrasonication of mixture composed of barium titanate, surfactant and chloroform, prior to its incorporation in the polymeric matrix would have led to a better dispersion of filler. The impact of the barium titanate particles on the silicone rubber properties was studied by comparing the results with those obtained on the similar samples prepared without filler as well as with a commercial acrylic sample, considered a high performance electromechanically active polymer, taken as reference.

To verify the moisture behavior, which can influence the stability of the characteristics of interest for the target application, the moisture sorption-desorption isotherms were registered in dynamic regime for the crosslinked composite films. A slight increase in the moisture sorption capacity occurs by raising the content of hydrophilic barium titanate (Figure 2). The maximum sorption capacity, registered around 80 % humidity, increases from 0.22 % in pure crosslinked PDMS to 0.76 % in the composite with 5% $BaTiO_3$, but the later value is lower as compared with that registered for commercial VHB sample (1.28 %) taken as reference. This diminished effect could be assigned to the surfactant coating barium titanate particles combined with the known tendency of the polysiloxane to migrate at the interface material-air, will lead to a surface richer in hydrophobic siloxane component.

Figure 2

Overall the isotherms correspond to a type III – specific for nonporous hydrophobic materials with weak interactions between sorbed and sorbing materials and show a small hysteresis loop. The slower water desorption rate as compared with sorption one, as the kinetic curves (not shown) revealed, is the explanation for this.

DSC experiments (Figure 6ESI) highlight the transitions occuring in the sample by temperature modification and associated heat capacity change (ΔC_p). It can be seen that all samples show glass transition around -120 - (-123) ^oC regardless of the molecular weight of PDMS and the filler content. The

samples based on polymers ABI and ABII exhibit nearly identical DSC traces, suggesting that $BaTiO_3$ particles have negligible influence on the thermal behavior of the samples. Thus, they show a reproducible exothermic peak at about -40 ^oC on the first and second heating curves assigned to melting, while on the cooling curve, an endothermic peak assigned to cold crystallization at about -70 ^oC develops. Instead, the sample based on higher molecular weight PDMS, ABIV, a heating crystallization process is visible around -92 ^oC, while the melting and cold crystallization occur at temperatures lower (-60 and -100 ^oC, respectively) as compared with samples based on polymers ABI and ABII. The high length of the polymer chain (Mn=142 000) and, as a result, the higher distance between crosslinks, permits occurrence of this process.

The thermogravimetric data (Figure 7ESI, Table 2) reveal the onset of degradation at higher temperatures for silicone samples (degradation onset at 397 ºC), in comparison with reference acrylic polymer sample (220 ºC). The thermal decomposition mainly occurs in a single step.

Table 2

The addition of barium titanate microparticles has a positive effect on the thermal resistance of the materials, as the onset temperature increases, although not very much, up to 437 ºC for sample with 5% $BaTiO_3$ (AB II MB5). The low value for the residue of degradation in inert atmosphere is due to breaking of the siloxane bond at high temperature and the formation of siloxane oligomers with low vaporization temperature and such chemical species are outgasing from the samples in the test crucibles.

The stress-strain tests (Figure 3, Table 3) reveal that the samples possess good flexibility and this property improves with the increase in the molecular mass of the siloxane used. The reinforcing effect of barium titanate particles is visible since samples with the highest content of filler (5%), ABII MB 5 and ABIV MB 5, have the largest value for stress for each siloxane polymer. However the increase in the molecular mass of the siloxane leads concurrently to a larger value of strain for sample ABIV MB 5, and this is due to longer free fragments of siloxane chains being capable of sliding past one another when stretched. In direct correlation, the Young's modulus values (Figure 8ESI) decrease with increasing flexibility, as siloxane films are known for low values of Young modulus [29]. Since for each sample the subsequent standard deviations were less than 2% of the average value, the graphs present only the average value for each type of film.

Figure 3

Table 3

The cyclic stress-strain curves registered up to 100 % of initial length strains, the samples were clearly different (Figure 4). The samples based on siloxane presented an elastic behaviour, with a clearly visible hysteresis loop only at the first strain-release cycle, probably due to the Mullins effect (the temporary phenomenon which disappears after a few cycles of solicitation when the elastomer response becomes completely stabilized and reproducible as long as the maximum stretching level is not exceeded) [30,31] and in the later strain cycles the siloxane chains are rearanged in the film and the difference between strain and release was smaller than 1% of the stress value at each point. The sample based on acrylic polymer presented a viscoelastic behaviour (Figure 9ESI) with nonlinear behaviour for cycles with strains above 50%; therefore the cycles were made with only 50% strain and a clear loss of strain energy by viscous component is visible in the curves.

Figure 4

Materials such as barium titanate and lead titanate have gained considerable interest both from scientific and application point of view. Such ceramics with the perovskite crystal structure possess excellent dielectric properties but also display poor mechanical performances. Polymers such as siloxanes possess very good flexibility but low dielectric permittivity. Therefore it is of interest to study the combination of ferroelectric fillers and siloxanes to obtain new materials with better properties. Since the materials were tested for the purpose of using in energy transducers, Figure 5 shows the graphs for the variation with frequency of the value of dielectric constant and dielectric loss at 20 ºC.

Figure 5

It is known that the dielectric responses of ceramic-polymer systems can be described by the logarithmic mixing rule and Maxwell–Garnett approximation [32-34]. There exists a distinct, although small, enhancement in dielectric constant with increasing filler content. However the increase of the ε' value is not as large as expected due to interactions between the layer of surfactant and the particles. The ε' values of the films decrease with increasing frequency. A significant drop in ε' occurs when the frequency reaches 10^3 Hz. In this case, the dipole relaxation in the composite films lags behind the change of applied fields. The characteristic relaxation peaks of the siloxane matrix in ε" curves (ABII MB0 and ABIV MB0) disappear with the introduction of barium titanate particles (Figure 5b,c) as this leads to the decrease of free volume in the polymer matrix and an increase of density of polar groups. A higher degree

of siloxane crosslinking would lead to increased values for permittivity since the free volume fraction would decrease but this would negatively affect the capability of the films to stretch with high percentages. However, the data presented in Figure 5 and Table 3 does not permit us to draw a clear conclusion about the influence of the molecular mass of the polymer on the dielectric constant of the crosslinked films.

The results of the breakdown field measurements show in general a decrease of dielectric strength when the barium titanate is incorporated and as its content embedded in silicone matrix increases (Table 3). For reference samples, these values are higher as compared with those reported in literature for room temperature vulcanization silicones [35,36]. Most of the values for our composites are comparable with those reported for polydimethylsiloxanes filled with encapsulated conductive polyaniline particles [7] or with commercial silicone Elastosil grafted with polar group but lower as compared with those obtained for Sylgard grafted with the same polar groups [37].

Based on the mechanical and dielectric characteristics, it can be estimated a parameter of interest for potential future application of such materials in electromechanical devices (actuation or harvesting). Thus, the electromechanical sensitivity, β, was calculated as the ratio between the dielectric permittivity (ε) at 5 kHz and the Young's modulus (Y) at 10% strain [13]. The dielectric permittivity values at this frequency being close enough (between 3.05 - 3.69), the electromechanical sensitivity is mainly influenced by the Young modulus value, which have a wider variation range (0.01 – 0.25 MPa) in the series of the prepared and analysed samples. It can be seen (Table 3) that in general the value of this parameter increases by incorporation of the filler and as the content of this rises but also at higher molecular mass of the polymeric matrix, the highest value being obtained for the sample ABIV MB5 (461.33 as compared with 0.04 MPa^{-1} determined for the commercial reference sample).

The maximal that can be harvested by a unit volume of material is proportional to the τ, defined by using formula (1) which can be considered as a merit parameter for the electrical properties of the material [31]. The obtained values are presented in Table 3. Unexpectedly, almost in all cases, this parameter decreases as the content of the ceramic filler rises. This is due the fact that the decrease in dielectric strength is more pronounced as compared with the increase in dielectric permittivity. The accentuated decrease in dielectric strength may be due, between others, to the imperfections within the material.

$$\tau = \varepsilon' E_{BS}^2 \quad (1)$$

For the sample ABIV MB0 with dielectric strength 102.2 kV/mm, this parameter related to the ability of harvesting energy, τ, has the largest value, i.e., 33110 kV^2/mm^2.

In another approach, the energy output can be estimated on the basis of both mechanical (uniaxial deformation) and electrical properties of tested samples [38] (see Supporting Information). The energy gained, E, from a cycle of operation (stretching and relaxing the variable generator) depends on the difference between the total capacitance in stretch state and relaxed state (Table 3). Although the values obtained by the two methods differ due to the different calculation bases, it seems that in both cases, the highest values were obtained when the matrix polymer had the greatest molecular weight and contained highest amounts of active filler. This is a very general trend; the exceptions to this could be assigned, between others, to the imperfections within the material.

The experimental values of the harvested energy, determined by using a home-made set-up (Figure 3ESI), expressed as peak-to-peak voltage (Figure 4ESI) are provided in Table 3. It can be seen that the obtained values range between 1.7 and 12 V and, as in the case of estimated ones, these are in general greater (2.3; 6.8; 8.5; 12; V) in the case of samples based on the polymer matrix with highest molecular mass (142 000 g/mol), than those collected (1.7; 3.2; 2.5; 7.6 V) in the case of the samples based on polymer with lower molecular mass (84 000 g/mol). Unfortunately, it cannot establish a correlation with the composition of the samples since these differ as thick (0.18-0.36 mm) and, as a result, the resistivity varies. What we can say on the basis of the above, is that the materials are suitable for converting mechanical energy in electric one.

4. Conclusion

Siloxane composites based on polydimethylsiloxane-α,ω-diols with different chain lengths as matrices and barium titanate powder as filler added in different percents (1, 2, and 5 wt%) were prepared and crosslinked in film forms. Samples without filler were prepared for comparison in similar conditions. DSC study reveals that the presence and amount of the filler do not affect the thermal transition of the crosslinked structures, these being influenced mainly by the polymer chain length. A slight increase in the thermostability of the samples due to the filler effect was emphasized by thermogravimetrical analysis. The presence of the barium titanate leads to increasing in moisture sorption in material. Considering the

intended use for energy conversion, the key parameters such as the ultimate strain, the elastic behaviour and the relaxation at repeated strain cycles were measured. In general, slight increases are registered both in mechanical parameters (Young modulus, tensile strength and elongation), although not regulate enough, and dielectric permitivity values by the incorporation of barium titanate as compared with samples without filler. The highest value for Young modulus was registered for the sample ABII MB5 based on the polymer with shortest chain and as a result the highest crosslinking density. Sample ABIV MB5 based on the longest chain and highest filler content showed the highest elongation value. The dielectric permitivity value increses from 3.20, 3.06, and 3.17 to 4.17, 3.85, and 3.98 respectively, by variation of the filler content from 0 to 5 wt%, differences being of 0.97, 0.79 and 0.81 in series ABI, ABII, and ABIV, respectively. The siloxane-based films show superior performance in elastic behaviour (in testing cycles) as compared with an acrylic commercial sample. Large variation in the electromechanical sensitivity (14.32 – 461.33 MPa^{-1}) and energy harvesting capacity (0.01-22.56 J) values estimated on the basis of the dielectric and mechanical characteristics were obtained, these depending mainly on the composition and structure of the composites as well as on film quality. The experimental peak-to-peak voltage values developed within composite film under a well-defined mechanical impact, measured for the two of the samples series, range between 1.7 and 12 V, these being more visible influenced by the molecular mass of the polymeric matrix. The complete characterization with emphasis on electro-mechanical behaviour of thus obtained cross-linked materials will be discussed in a forthcoming publication.

Acknowledgments: The work presented in this paper is developed in the context of the project PolyWEC (www.polywec.org, prj. ref. 309139), a FET-Energy project that is partially funded by the 7th Framework Programme of European Community. Support by the COST Action (MP1003) “European Scientific Network for Artificial Muscles (ESNAM)”, through Short-Term Scientific Missions COST-STSM-MP1003-14671 and 14672, and PERCRO Laboratory - TeCIP Institute - Scuola Superiore Sant'Anna Pisa Italy for technical support are also gratefully acknowledged. The authors thank to Rocco Vertechy and Marco Fontana from Scuola Superiore Sant’Anna, Pisa for helpful discussions.

References

1. Gharavi N, Razzaghi-Kashani M, Golshan-Ebrahimi N. Effect of organo-clay on the dielectric

relaxation response of silicone rubber. Smart Mater Struct 2010;19(2):025002.

2. Vertechy R, Fontana M, Rosati Papini G P, Forehand D. In-tank tests of a dielectric elastomer generator for wave energy harvesting. Proc. SPIE 9056, Electroactive Polymer Actuators and Devices (EAPAD) 2014, 90561G (March 8, 2014); doi:10.1117/12.2045046.
3. Moretti G, Forehand D, Vertechy R, Fontana M, Ingram D. Modelling of an oscillating wave surse. In Proc. of the ASME 2014 33rd International Conference Converter with Dielectric Elastomer Power Take-Off on Ocean, Offshore and Arctic Engineering, OMAE2014-23559 (2014).
4. Tuncer E, Isidor S. Chapter 11, Industrial Applications Perspective of Nanodielectrics, p. 321. In: Nelson J. Keith (Ed.), Dielectric Polymer Nanocomposites, Springer, New York, NY, USA, 2009, http://info.ornl.gov/sites/publications/files/Pub15336.pdf
5. Koulouridis S, Kiziltas G, Zhou Y, Hansford DJ, Volakis JL. Polymer–ceramic composites for microwave applications: fabrication and performance assessment. IEEE T Microw Theory 2006;54(12):4202–4208.
6. Gubbels F, De Jaeger R, Gleria M. Chapter 2. Silicones in Industrial Applications Inorganic Polymers, Nova Science Publishers, 2007. p. 61-162.
7. Risse S, Kussmaul B, Krüger H, Waché R, Kofod G. DEA material enhancement with dipole grafting PDMS network. Proc SPIE 7976, Electroactive Polymer Actuators and Devices (EAPAD) 2011, 79760N.
8. Racles C, Cazacu M, Fischer B, Opris DM. Synthesis and characterization of silicones containing cyanopropyl groups and their use in dielectric elastomer actuators. Smart Mater Struct 2013;22:000000 (10 pages).
9. Carpi F, Gallone G, Galantini F, De Rossi D. Chapter 6. Enhancing the dielectric permittivity of elastomers, p. 60. In: Dielectric Elastomers as Electromechanical Transducers: Fundamentals, Materials, Devices, Models and Applications of an emerging electroactive Polymer Technology, Carpi F, De Rossi D, Kornbluh R, Pelrine R, Sommer-Larsen, P. (Eds.), Elsevier Ltd., 2008.
10. Wang Z, Nelson J. Keith, Miao J, Linhardt R J, Schadler Linda S, Hillborg H, Zhao Su. Effect of high aspect ratio filler on dielectric properties of polymer composites: a study on barium titanate fibers and graphene platelets. IEEE Trans Dielectr Electr Insul 2012;19(3):960–967.

11. Yin Y, Chang X. Chapter 10. Ocean Engineering Application of Nanocomposites. In: Multifunctional Polymer Nanocomposites, Jinsong Leng, Alan K. T. Lau (Eds.), CRC Press, Taylor and Francis Group, Boca Raton, FL, 2011.

12. Sebastian MT, Jantunen H. Polymer-ceramic composites of 0–3 connectivity for circuits in electronics: a review. Int J Appl Ceram Technol 2010;7(4):415–434.

13. Zhao H, Wang D-R, Zha J-W, Zhao J, Dang Z-M. Increased electroaction through a molecular flexibility tuning process in TiO_2–polydimethylsilicone nanocomposites. J Mater Chem A 2013;1:3140–3145.

14. Huang C, Zhang QM. Fully functionalized high-dielectric-constant nanophase polymers with high electromechanical response. Adv Mater 2005:17:1153–1158.

15. Chon J, Ye S, Cha KJ, Lee SC, Koo YS, Jung JH, Kwon YK. High-k dielectric sol-gel hybrid materials containing barium titanate nanoparticles. Chem Mater 2010;22:5445–5452.

16. Hanemann Th, Schumacher B. Realization of embedded capacitors using polymer matrix composites with barium titanate as high-k-active filler. Microsyst Technol 2012;18:745–751.

17. Choudhury A. Dielectric and piezoelectric properties of polyetherimide/$BaTiO_3$ nanocomposites. Mater Chem Phys 2010;121:280–285.

18. Popierlarz R, Chiang CK, Nozaki R. Dielectric properties of polymer/ferroelectric ceramic composites from 100 Hz to 10 GHz. Macromolecules 2001;34:5910–5915.

19. Arora S, Ghosh T, Muth J. Dielectric elastomer based prototype fiber actuators. Sens Actuators A 2007;136(1):321–328.

20. Kofod G, Kornbluh R, Pelnine R, Sommer-Larsen P. Actuation response of polyacrylate dielectric elastomers. J Intell Mater Syst Struct 2003;14:787-793.

21. Wissler M, Mazza E. Mechanical behavior of an acrylic elastomer used in dielectric elastomer actuators. Sens Actuators A 2007;134(2):494–504.

22. Nayak S, Chaki, Khastgir D. Development of poly(dimethylsiloxane)/$BaTiO_3$ nanocomposites as dielectric material. Adv Mater Res 2013;622-623:897–900.

23. Hanemann Th, Gesswein H, Schumacher B. Development of new polymer–$BaTiO_3$-composites with improved permittivity for embedded capacitors. Microsyst Technol 2011;17:195–201.

24. Lin Z-H, Yang Y, Wu JM, Liu Y, Zhang F, Wang ZL. $BaTiO_3$ nanotubes-based flexible and

transparent nanogenerators. J Phys Chem Lett 2012;3:3599−3604.

25. Brochu P, Pei Q. Advances in dielectric elastomers for actuators and artificial muscles. Macromol Rapid Commun 2010;31:10–36.

26. Cazacu M, Marcu M. Silicone Rubber IX. Contributions to polydimethylsiloxane-□□□-diols synthesis by heterogeneous catalysis. Macromol Rep A 1995;32:1019–1029.

27. Cazacu M, Ignat M, Racles C, Cristea M, Musteata V, Zarnescu G, Lipcinski D. Well-defined silicone/titania composites with good performances in actuation and energy harvesting. Compos Mater 2014;48:1533-1545.

28. Arellano M, Manas-Zloczower I, Feke DL. Assessment of the dispersibility of surfactant-treated titanium dioxide powders for compounding with polyethylene. Polym Compos 1995;16(6):489–494.

29. Ogawa T, Takei S, Willson CG. Ultraviolet curable branched siloxanes as low-k dielectrics for imprint lithography. J Vac Sci Technol B 2013;31:011601–011606.

30. Mullins L. Softening of rubber by deformation. Rubb Chem Technol 1969;42:339-362.

31. Vertechy R, Fontana. M, Stiubianu G, Cazacu M. Open-access dielectric elastomer property database, Proc. SPIE 9056, Electroactive Polymer Actuators and Devices (EAPAD), 2014, 90561R (March 8, 2014); doi:10.1117/12.2045053.

32. Dang Z-M, Shen Y, Nan C-W. Dielectric behavior of three-phase percolative Ni–$BaTiO_3$/polyvinylidene fluoride composites. Appl Phys Lett 2002;81:4814–4816.

33. Cheng K-C, Lin C-M, Wang S-F, Lin S-T, Yang CF. Dielectric properties of epoxy resin-barium titanate composites at high frequency. Mater Lett 2007;61:757–760.

34. Li YC, Tjong SC, Li RKY. Dielectric properties of binary polyvinylidene fluoride/barium titanate nanocomposites and their nanographite doped hybrids. eXPRESS Polymer Letters, 2011;5(6):526–534.

35. Danikas MG. On the breakdown strength of silicone rubber. IEEE Trans Dielectr Electr Insul 1994;1(6):1196-1200.

36. Molberg M, Crespy D, Rupper P, Nüesch F, Månson J-AE, Löwe Ch, Opris DM. High breakdown field dielectric elastomer actuators using encapsulated polyaniline as high dielectric constant filler. Adv Funct Mater 2010;20:3280–3291.

37. Risse S, Kussmaul B, Krüger H, Kofod G. A versatile method for enhancement of electromechanical sensitivity of silicone elastomers. RSC Advances 2012;2:9029–9035.

38. Chiba S, Waki M, Kornbluh R, Pelrine R. Current status and future prospects of power generators using dielectric elastomers. Smart Mater Struct 2011:20: 124006 (7pp).

Figure Captions

Scheme 1. Crosslinking of polydimethylsiloxane-α,ω-diols

Figure 1. SEM images in cryo-fractured section: a) barium titanate microparticles; b) ABI MB5; c) ABII MB5; d) ABIV MB5

Figure 2. Sorption/desorption isotherms for the prepared samples as compared with a reference sample

Figure 3. Stress-strain behaviour of the composite films

Figure 4. Cyclic stress-strain tests on the crosslinked composite films

Figure 5. Dielectric spectroscopy results for the tested samples with dielectric constant and dielectric loss values at: (a) AB I at T= 20 ºC; (b) AB II at T= 20 ºC; (c) AB IV at T = 20 ºC

Table 1

Table 1. Feed compositions in pph used for the preparation of the dielectric elastomers (100 pph PDMS, 8 pph crosslinker, MTAS)

Sample	PDMS/100 pph			$BaTiO_3$,	Surfactant,
	Polymer code	M_n	$I=M_w/M_n$	pph	pph
ABI MB0	**ABI**	84000	1.4	0	0
ABI MB1	**ABI**			1	1
ABI MB2	**ABI**			2	2
ABI MB5	**ABI**			5	5
ABII MB0	**ABII**	55000	1.4	0	0
ABII MB1	**ABII**			1	1
ABII MB2	**ABII**			2	2
ABII MB5	**ABII**			5	5
ABIV MB0	**ABIV**	142000	1.7	0	0
ABIV MB1	**ABIV**			1	1
ABIV MB2	**ABIV**			2	2
ABIV MB5	**ABIV**			5	5

Table 2

Table 2. Thermogravimetrical data for the samples tested

Sample	T_{onset}	T_{end}	Peak (ºC)	Residual mass (%)
AB II MB 0	397	549	491	7.0
AB II MB 1	419	614	499	13.8
AB II MB 2	430	609	546	9.4
AB II MB 5	436	630	582	8.4
Reference sample	220	540	380	3.0

Table 3-r

Table 3. The main parameters of the mechanical and dielectric tests

Sample	Y[a], MPa	ó[b], MPa	å[c], %	å` (10 Hz, 20 °C)	å`` (10 Hz, 20 °C)	E_{BS} [e], kV/mm	â[d], MPa^{-1}	ô[f] $x10^3$ kV^2/mm^2	E,[g] J	Film thick., mm	U_{vv},[h] V
ABI MB0	0.18	0.25	480	3.20	0.04	n.d.[i]	-	-	-	0.34	2.5
ABI MB1	0.15	0.33	621	3.26	0.48	55.55	21.47	10.060	9.49	0.22	3.2
ABI MB2	0.23	0.50	795	4.00	1.14	44.76	16.04	8.014	17.54	0.28	1.7
ABI MB5	0.27	0.32	516	4.17	0.44	13.12	14.32	0.718	0.43	0.31	7.6
ABII MB0	0.05	0.35	452	3.06	0.01	n.d.[i]	-	-	-	-	-
ABII MB1	0.02	0.29	330	3.26	0.05	n.d.[i]	-	-	-	-	-
ABII MB2	0.01	0.30	585	3.55	0.01	n.d.[i]	-	-	-	-	-
ABII MB5	0.18	0.40	249	3.85	0.01	8.84	19.72	0.301	0.01	-	-
ABIV MB0	0.25	0.18	543	3.17	0.15	102.20	12.68	33.110	6.24	0.34	8.5
ABIV MB1	0.07	0.20	780	3.57	0.51	52.64	50.90	9.892	18.37	0.36	12.0
ABIV MB2	0.06	0.23	641	3.73	0.68	23.31	58.39	2.027	2.37	0.18	6.8
ABIV MB5	0.01	0.32	850	3.98	0.52	39.25	461.33	6.131	22.56	0.31	3.3
Reference	0.06	0.58	950	2.89	3.30	48.17	0.04	-	-	-	-

a – Young's modulus at 10% strain; b – Stress at break; c – elongation at break; d – electromechanical sensitivity [13]; e – dielectric strength; f – estimated energy harvested [31]; g - energy gained estimated according to ref. [38]; h - peak to peak measured voltage (Figure 5ESI); i - no determined because tie films were thick and the breakdown field was not achieved up to 10 kV, maximum voltage of our source.

Scheme 1

Click here to download high resolution image

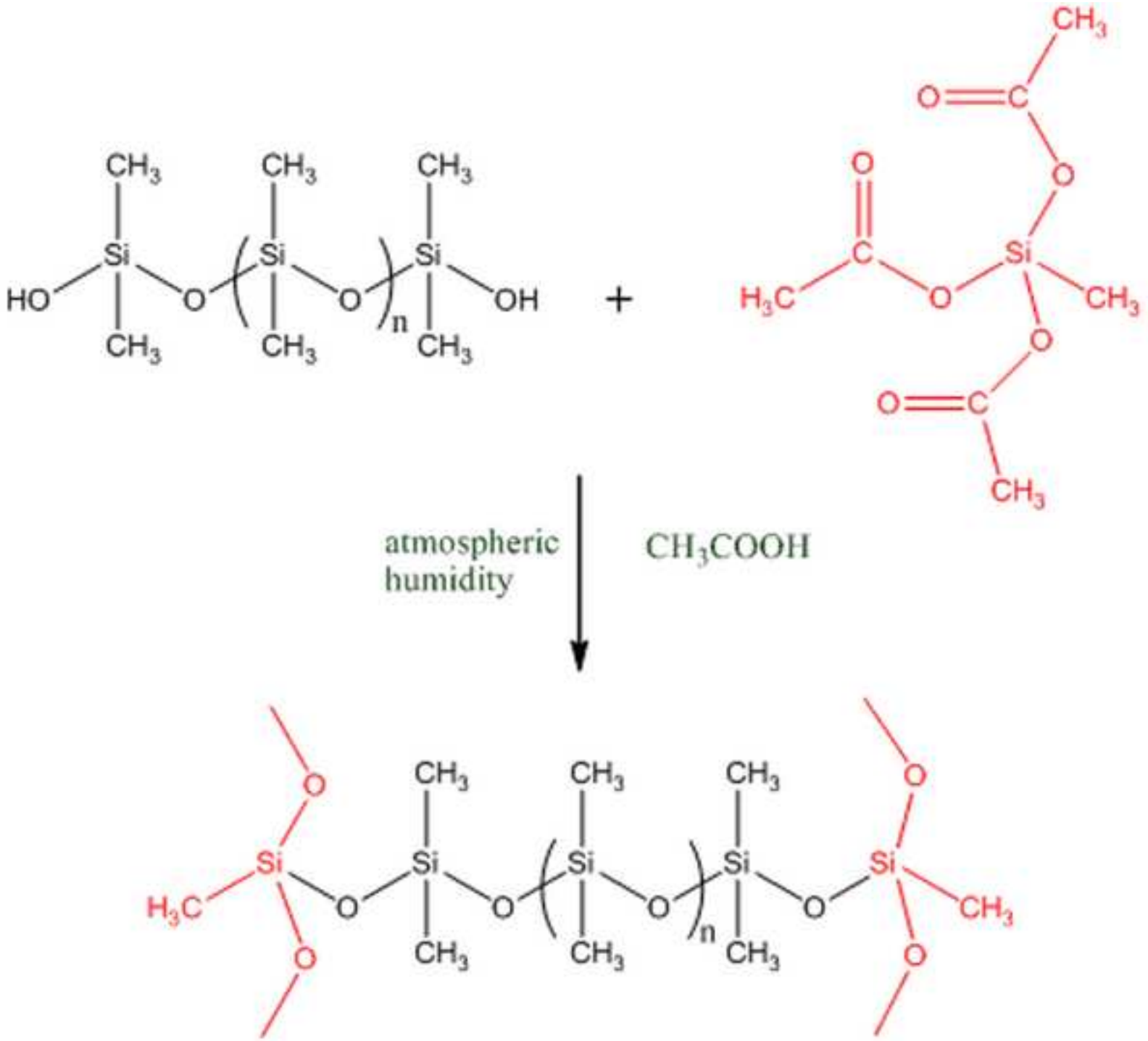

Figure 1

Click here to download high resolution image

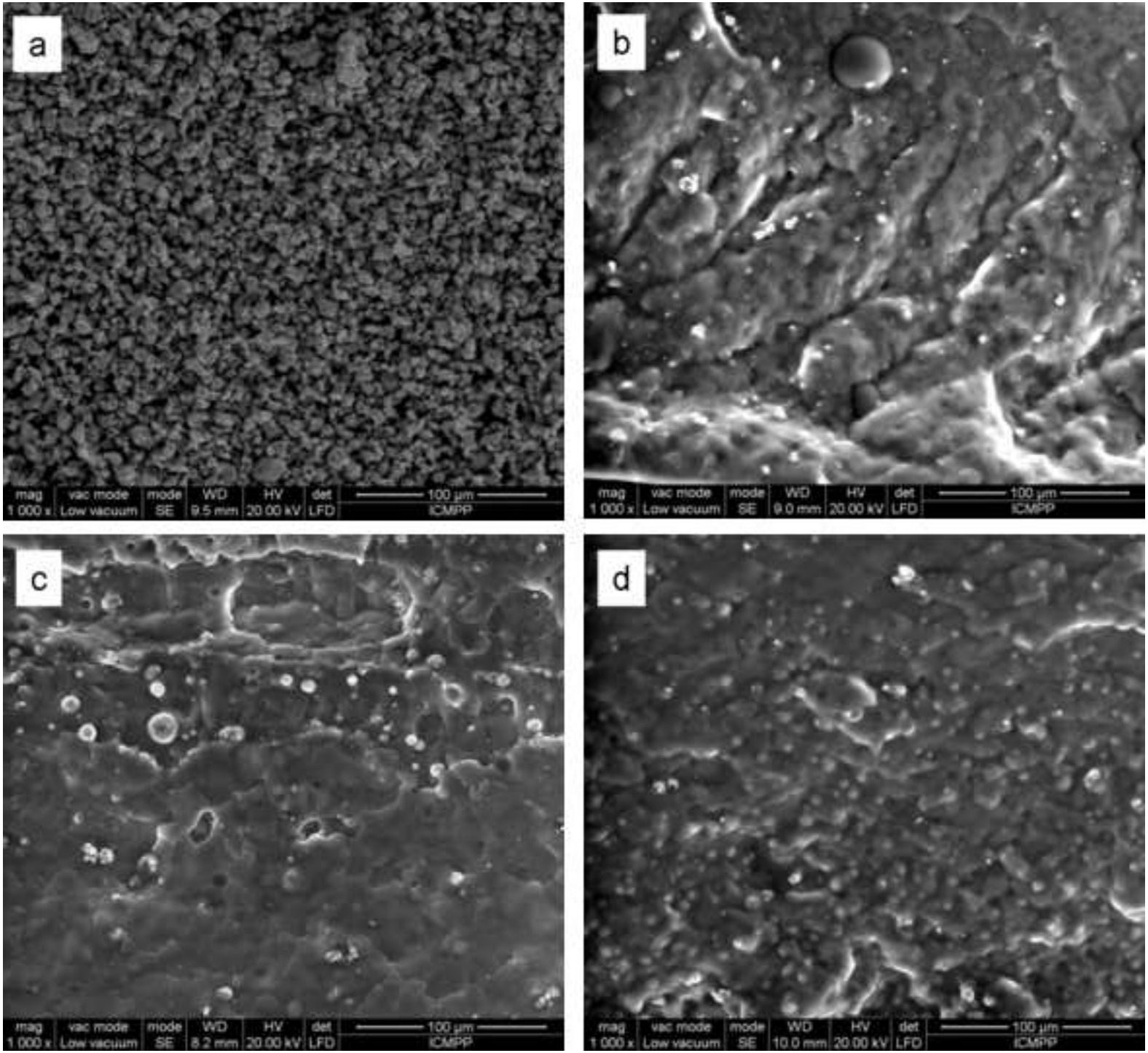

Figure 2

Click here to download high resolution image

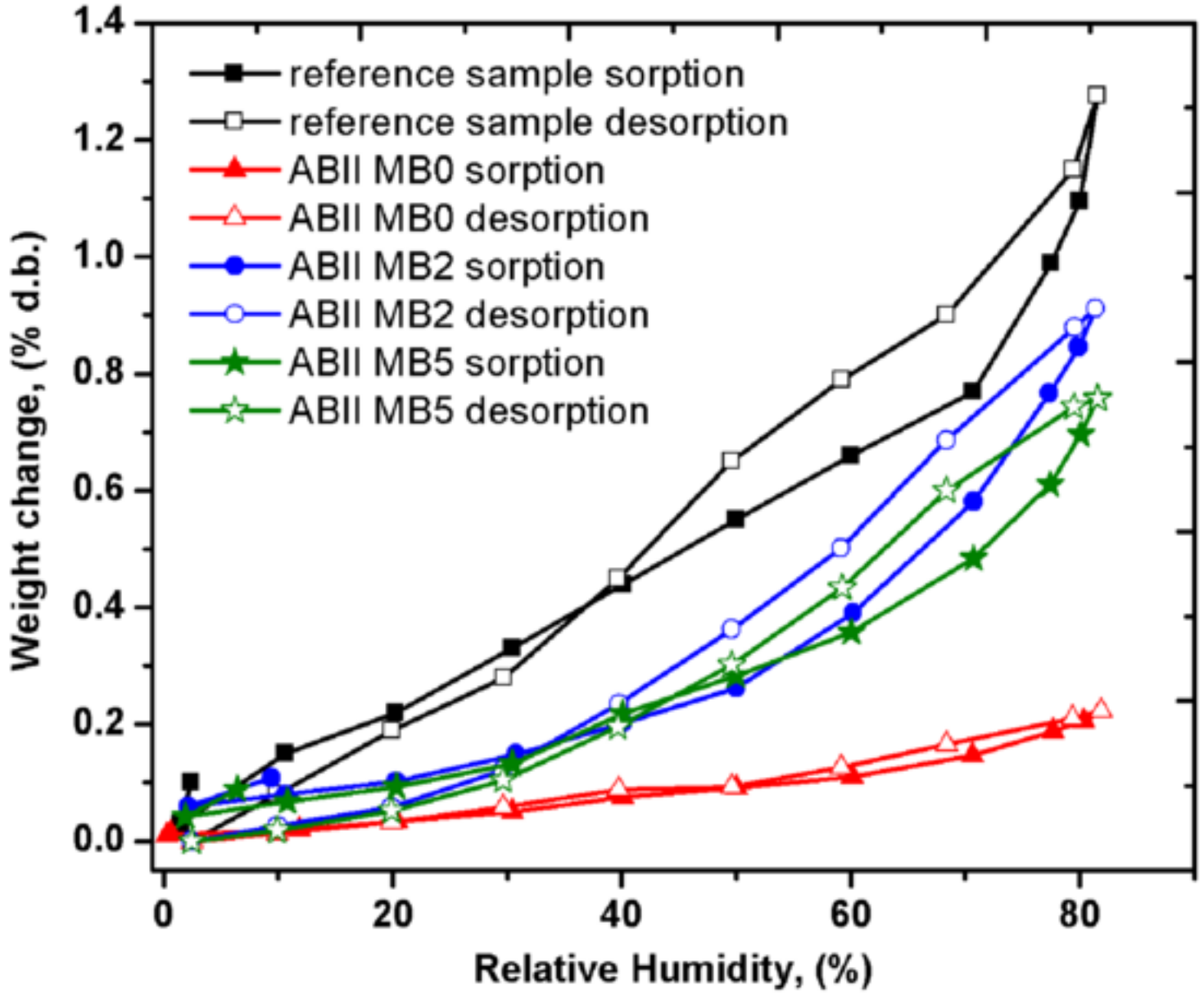

Figure 3

Click here to download high resolution image

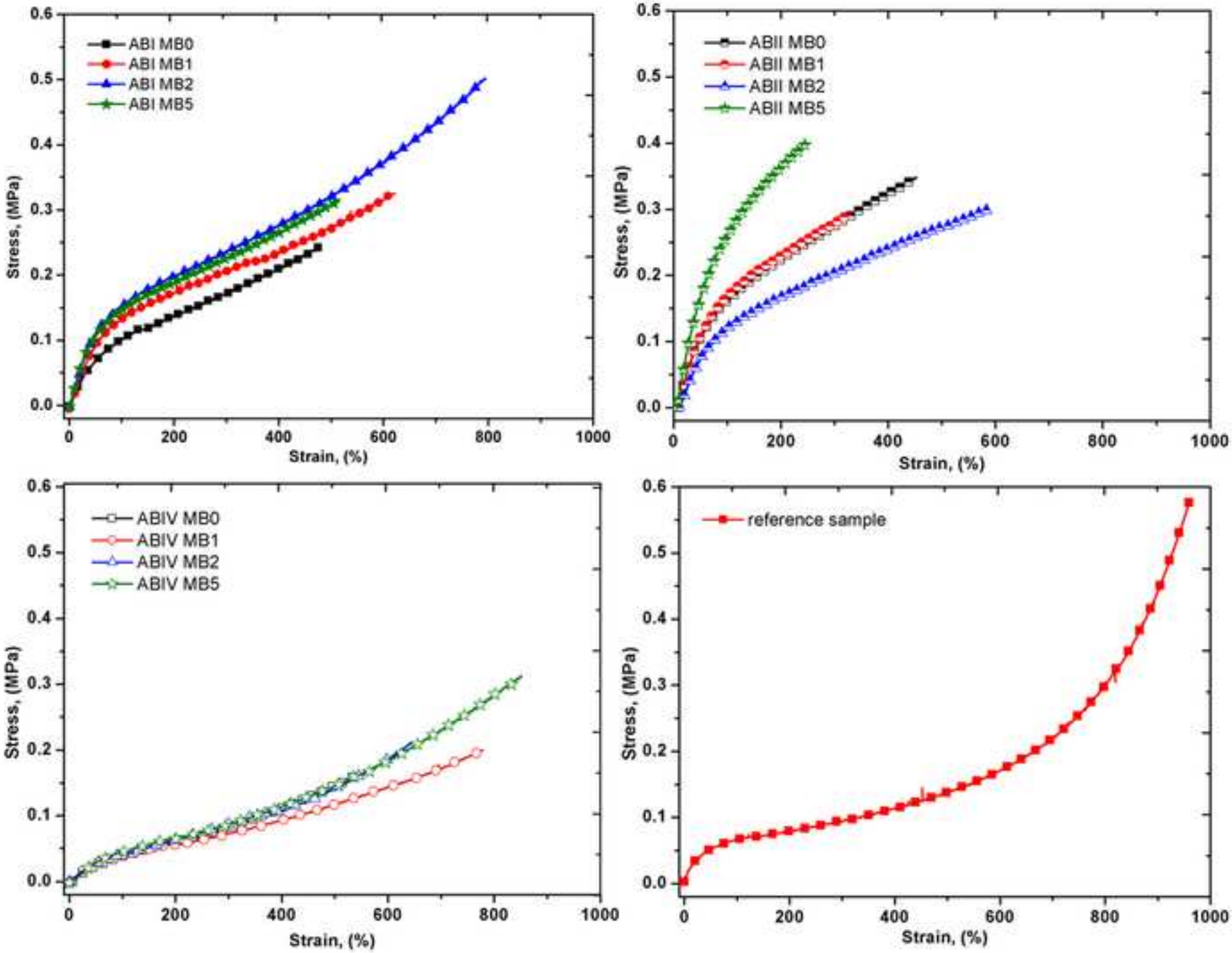

Figure 4-r

Click here to download high resolution image

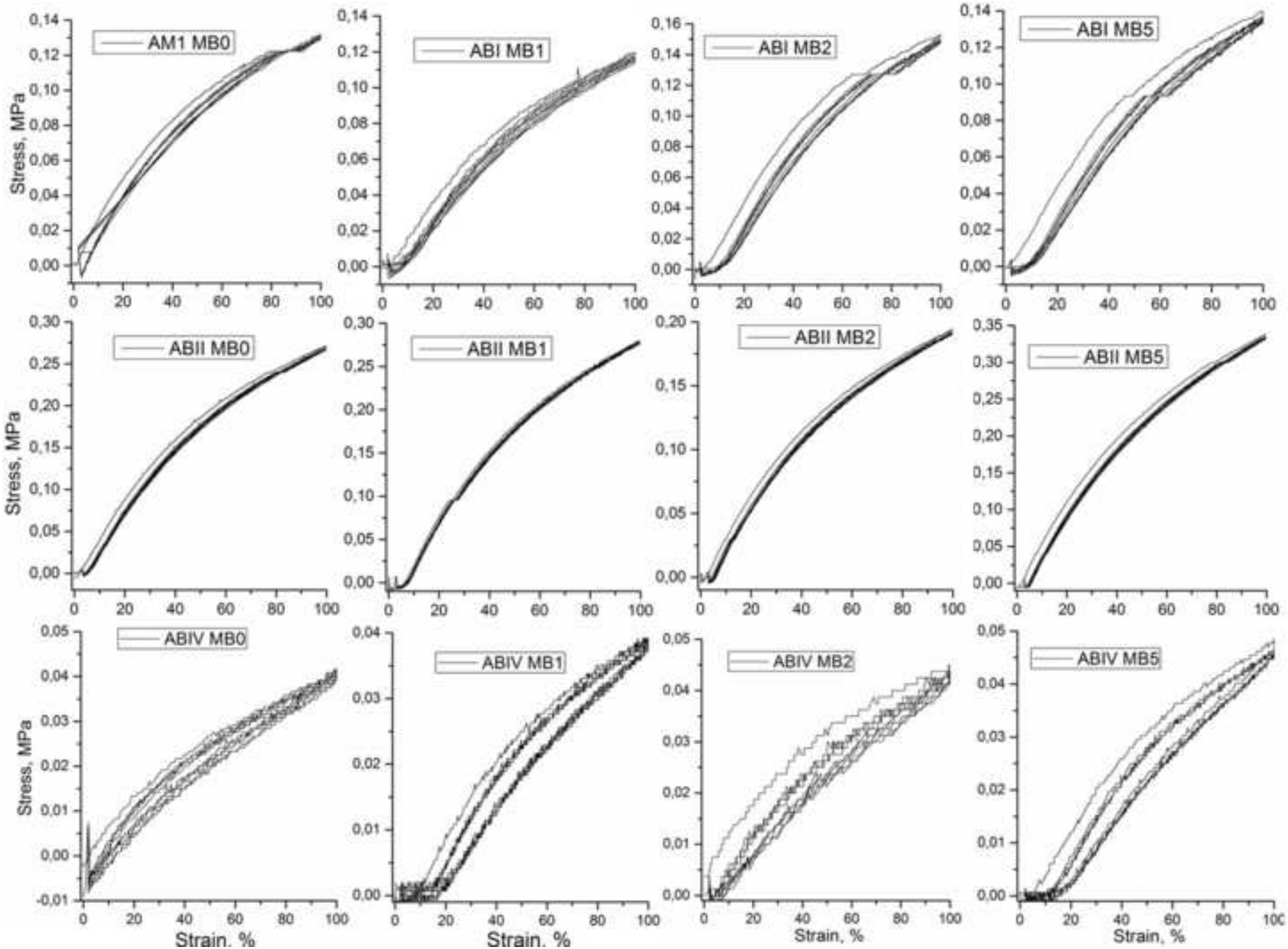

Figure 5-r

Click here to download high resolution image

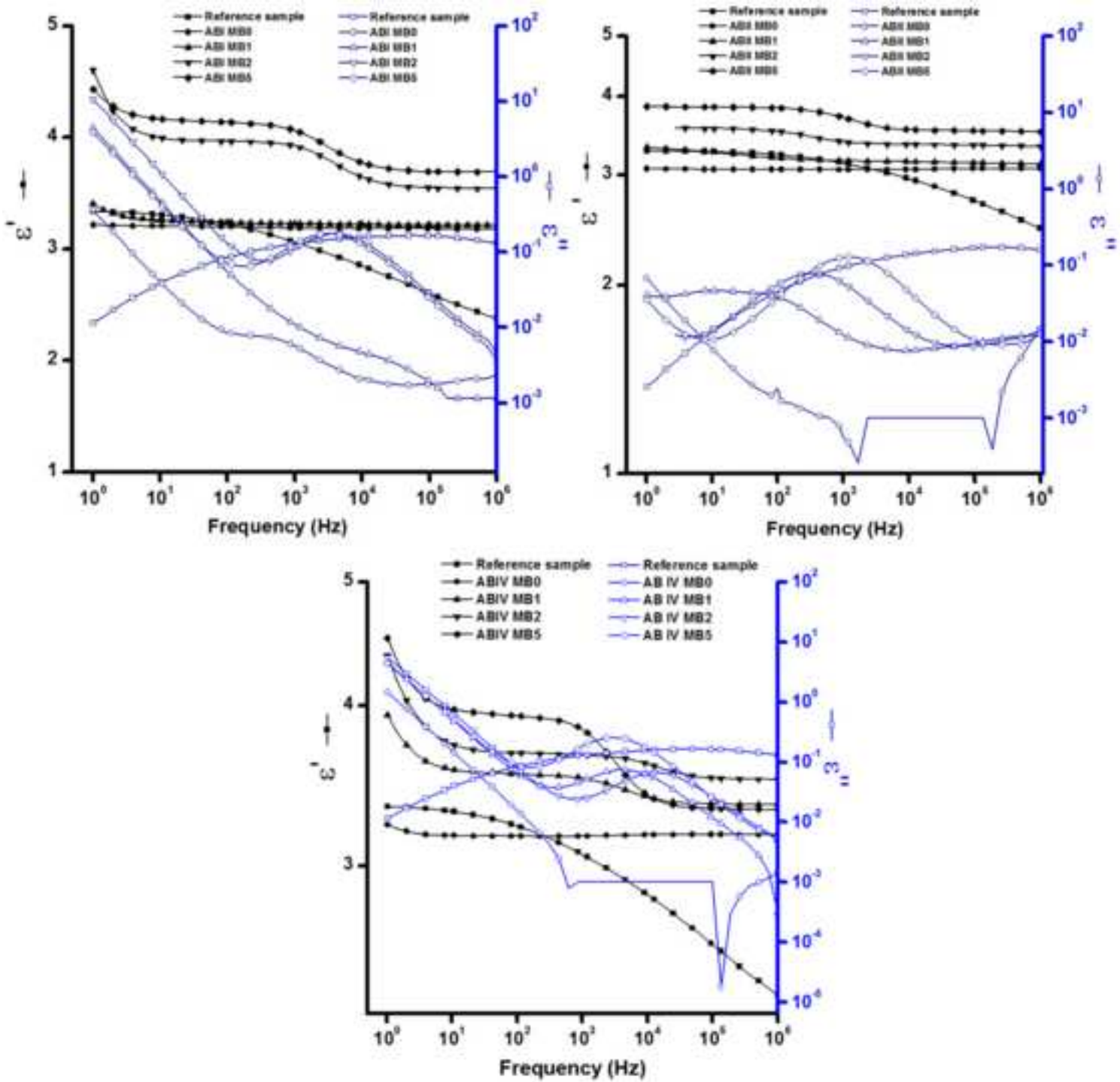

Supporting information

Click here to download e-Component (Video, Audio, Supplemental Text, etc.): Supplementary information-r.doc